Aggregation-Based Power Fluctuation Mechanisms for Offshore Wind Power Clusters During Typhoons

Jiale Luo
College of Electrical Engineering, Shanghai University of Electric Power, Shanghai, China
770924331@qq.com

Xiangjing Su
Offshore Wind Power Research Institute, Shanghai University of Electric Power, Shanghai, China
xiangjing_su@126.com

Shiqu Xiao
College of Electrical Engineering, Shanghai University of Electric Power, Shanghai, China
xiaoshiquovo@foxmail.com

Yunhui Tan
College of Electrical Engineering, Shanghai University of Electric Power, Shanghai, China
2944792314@qq.com

Yang Liu
Offshore Wind Power Research Institute, Shanghai University of Electric Power, Shanghai, China
liuyang_ssun@163.com

Yang Fu
Offshore Wind Power Research Institute, Shanghai University of Electric Power, Shanghai, China
mfudong@126.com

***Abstract*—Frequent typhoon disasters pose operating threats on modern power systems, while there is a lack of mechanism for modeling the impact on the fluctuating power of offshore wind farm (OWF) clusters. To fill this research gap, a Wind Delay Spatial Aggregation (WDSA) model is proposed to achieve ultra-short-term power fluctuation modeling of OWF clusters under typhoons. Firstly, on the wind farm side, an available installed capacity coefficient (AICC) is designed for each wind farm to represent the impact of typhoons on the shutdown of wind turbines. Secondly, the time delay caused by wind direction is introduced into the unidirectional aggregation model. Finally, a case study is conducted using the actual output of OWF clusters in the sea areas near Jiangsu during typhoon periods in 2023. Compared with the existing models, the proposed WDSA model accurately analyze the power attenuation and recovery process, and the overall RMSE has increased by 4.32%. The ablation experiment indicated that the NRMSE of the proposed model is only 7.41%, and the sensitivity analysis determined the optimal values of the model parameters.**

Keywords*—typhoon, offshore wind power cluster, available installed capacity

I. Introduction

In the goal of China's "dual carbon" strategy, offshore wind farms (OWFs) have become core carriers in renewable energy transitions. However, the threat of typhoon poses great technical challenges to the assessment of OWF operating conditions, which causes the power fluctuations of main grids. Currently, the complete shutdown strategy under typhoon disasters cannot meet the power supply demands of high-RES integrated power grids, while the power fluctuation analysis mechanism of offshore wind clusters is still unclear[1],[2].

Many researches have been conducted on the impact of wind characteristics on wind power delivery. References [3] and [4] propose a new topological structure to address the issue of uneven wind speed, aiming to improve the performance and efficiency of offshore wind farm systems; Reference [5] proposes a novel two-tier wind power time series model. By considering the wind power fluctuation characteristics of wind power at the first time point of each day, this model realizes the characterization of the intraday wind power fluctuation process. However, existing studies focus on analyzing the impact of wind speed on the power output of wind farms under normal operating conditions, and fail to descript the impacts of turbines shutdown on the OWF power.

An aggregation model is proposed in [6] to conduct cluster analysis by accumulating OWF powers. An improved Support Vector Clustering (SVC) algorithm is proposed to improve the aggregation model [7]. Reference [8] designs a multi-objective optimization algorithm that fully considers wind speed disturbances and system faults, which is applied to the improved aggregation model for large-scale power system stability research. In [9], a modeling method for wind speed with the same torque in a wind farm is proposed, and a wind speed combination model is established through the K-means clustering method. However, the above studies on wind power aggregation effect fail to consider the scattered spatial distribution of OWFs and the time-lag characteristics of power fluctuations when typhoons pass through.

Therefore, this paper introduces a novel Wind Delay Spatial Aggregation (WDSA) model for power fluctuation analysis for OWF clusters under typhoons. By considering factors such as unstable wind speed and sudden wind direction changes caused by typhoons, an available installed capacity coefficient (AICC) for each wind farm is formulated, and a dynamic mapping function between typhoon disturbances and power fluctuations is established. In terms of clusters, considering the geographical locations and wind directions among wind farms, the time delay calculated by wind direction is introduced. A power aggregation power function for OWF clusters is constructed. This function analyzes the relationship between typhoons and power fluctuations in clusters. Finally, simulation experiments of OWF clusters in the sea area near Jiangsu have proved the validity of the proposed model.

II. Power Modeling of Single-Order OWF Under Typhoon Action

A. Traditional Benchmark Model

Traditional models commonly adopt the direct mapping approach of the conventional wind-speed-to-power curve, which is widely used in wind power forecasting studies [10]. For ease of analysis, the overall spacetime field $\Gamma = \Omega \cup [0,T]$ is defined mathematically. Physically, what covers the cluster area of wind farms is the wind flow field with temporal and spatial variations. In Γ, both wind speed and wind direction vary in time and space. Since air is a continuum, the wind flow with such spatiotemporal variations in Γ can be regarded as a wind speed flow field. The scalar wind speed of spatiotemporal distribution is expressed as:

XXX-X-XXXX-XXXX-X/XX/$XX.00 ©20XX IEEE
979-8-3315-8138-1

$$v_{\text{wind}}((x,y),t) \quad ((x,y),t) \in \Gamma \tag{1}$$

Substituting the coordinates of wind farm i (x_i,y_i), the wind speed of wind farm i is simplified to a function of time:

$$v_{\text{wind},i}(t) = v_{\text{wind}}((x_i, y_i), t) \tag{2}$$

From the relationship between wind speed and power conversion, it is known that the power of a wind farm is a cube function of wind speed. Therefore, the wind speed waveforms of representative wind farms $v_{\text{wind}}((x^{\text{rep}}, y^{\text{rep}}), t)$ can be used to calculate the calculated power waveform of this wind farm as:

$$\mathrm{P^{rep}(t) = K_P^{rep}[v_{wind}((x^{rep}, y^{rep}), t)]^3} \tag{3}$$

where K_P^{rep} represents the wind-power conversion coefficient of a representative wind farm.

Performing Fourier transform on the power waveform of a representative wind farm can decompose it into a DC component $P_{\text{const}}^{\text{rep}}$ and a pure AC component $P_{var}^{\text{rep}}(t)$:

$$P^{\text{rep}}(t) = P_{\text{const}}^{\text{rep}} + P_{var}^{\text{rep}}(t) \tag{4}$$

This model can only reflect the ideal power changes caused by wind speed, but cannot characterize the capacity attenuation phenomenon resulting from the mass shutdown of wind turbines during typhoon passage.

B. Improved Single Wind Field Power Modeling

Traditional models struggle to accurately capture the dynamic loss of available capacity caused by adverse wind conditions during typhoon passage. To address this, we propose a typhoon-specific AICC, denoted as δ_{A}. This coefficient quantifies the proportion of a wind farm's actual operable capacity relative to its total theoretical installed capacity under specific typhoon-induced wind conditions.

The core of this model lies in establishing a mapping relationship between key typhoon wind parameters and the probability of turbine shutdowns, thereby constructing a comprehensive turbine failure outage rate model under typhoon influence. The failure rate considering typhoon impacts can be expressed as:

$$w_{\text{wind}} = \begin{cases} 1 & v_t \le v_{\text{cri}} \\ C_{\text{p}}\left(\frac{v_t^2}{v_{\text{cri}}^2} - 1\right) & v_t > v_{\text{cri}} \end{cases} \tag{5}$$

where w_{wind} is the failure rate impact factor considering the influence of typhoons, v_t is the wind speed at time t , and v_{cri} is the critical wind speed.

Algorithm 1: Calculation Method of δ_{A} Based on Wind Speed Failure Rate and Monte Carlo Simulation （MCS）

1.Calculate the wind speed failure rate through formula (3).

2.Perform MCS for the i-th wind turbine in the wind farm to generate random number $rand_n$.

3.Judge the state:

Wind turbine state $s_i = \begin{cases} 1, & if \quad rand_{\text{n}} < w_{\text{wind}} \\ 0, & if \quad rand_{\text{n}} \ge w_{\text{wind}} \end{cases}$

4.Calculate the arithmetic mean $\mathrm{E}[s_i]$ of the state values (0 or 1) from n simulations for the i-th wind turbine.

5.End the wind turbine loop.

6.Calculate δ_A of the wind farm:

Assume the wind farm consists of k wind turbines of the same type, each with a rated capacity of P_{rated}.

Theoretical total installed capacity of the wind farm:

$$C_{\text{total}} = k * P_{\text{rated}}$$

Expected available capacity of the wind farm:

$$E_{\text{c}} = \sum_{i=1}^{k} E[s_i] * P_{\text{rated}}$$

AICC: $\delta_{\text{A}} = \frac{E_c}{C_{\text{total}}}$

Then, $\delta_{\text{A}} = \frac{\sum_{i=1}^{k} \mathrm{E}[s_i]}{k}$

7.return δ_{A}

The corresponding δ_{A} is obtained through the calculation shown in Algorithm 1. This dynamic will be introduced into the subsequent wind farm power function as a key input parameter.

C. Power Function of a Single OWF in Typhoons

The waveform of the representative power $P_1(t)$ of a single wind farm can be decomposed into a frequency spectrum via FFT, and the FFT result can be divided into two parts:

$$P_1(t) = P_{1,\text{const}} + P_{1,\text{var}} \tag{6}$$

where $P_{1,const}$ is the constant component, and $P_{1,\text{var}}(t)$ is a set of alternating components with an average value of zero.

The representative power $P_1(t)$ of a wind farm typically exhibits multi-time-scale variation characteristics. FFT decomposes the power fluctuation time series into a superposition of multiple sinusoidal functions with different frequencies, where each sinusoidal function corresponds to a specific frequency component. Based on the power spectral density analysis, the main frequency components are selected to construct the model. The decomposed $P_1(t)$ is expressed as follows:

$$P_1(t) = P_{1,\text{const}} + \sum_{q=1}^{s} P_{1,q,\text{max}} \sin(2\pi f_q t - \theta_q) \tag{7}$$

where s is the number of power samples; $P_{1,q,\text{max}}$ is the maximum value of the q-th power sample; f_q is the frequency of this frequency component, and θ_q is the phase angle of this frequency component.

By introducing the improved δ_{A} into the alternating components, a three-level mapping power $P_{\text{wind},1}(t)$ function for a single wind farm under typhoon conditions is proposed, as shown in the following formula:

$$P_{\text{wind},1}(t) = P_{1,\text{const}} + \delta_{\text{A}} \sum_{q=1}^{s} P_{1,q,\text{max}} \sin(2\pi f_q t - \theta_q) \tag{8}$$

III. Spatio-temporal Aggregation Model for OWF Clusters

A. Unidirectional Aggregation Model of Single OWF

For an actual wind-farm cluster, the spatiotemporal variation wind described by wind speed $v_{\text{wind}}((x,y),t)$ is a complex flow field. Moreover, the spatial layout of the farms is irregular and further distorted by terrain. Under such a realistic wind field it is extremely difficult to establish a deterministic link between the power waveform of a single farm and that of the whole cluster.

Operational records and wind-resource assessments show, however, that the cluster exhibits a prevailing wind direction. Aligning the x-axis with this direction allows the spatiotemporally varying wind field $v_{\text{wind}}((x,y),t)$ to be reduced to a one-dimensional flow $v_{\text{wind}}(x,t)$. As illustrated in Fig. 1, five wind farms WF_i are then distributed along this dominant direction.

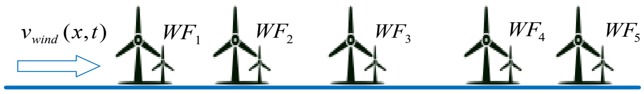

Fig.1 1-dimensional spatial distribution of each wind farm under the dominant wind direction

Along the prevailing wind direction, the flow successively passes each wind farm, inducing correlation between the power waveforms of adjacent farms. Taking the actual cluster as an example, the five wind farms are aligned with this direction; the pairwise correlations of their power waveforms are listed in Table I.

Table I confirms that the power waveforms of adjacent wind farms along the prevailing direction are indeed correlated. Building on this observation, a unidirectional aggregation model can be developed to investigate how the power waveform evolves from an individual wind farm to the entire cluster along the dominant flow.

Inspired by the travelling-wave concept, the one-dimensional wind field $v_{\text{wind}}(x,t)$ is treated as a wave propagating at a constant velocity v_{travel}. Assuming that the coordinate of wind farm i, which is distributed along the x-axis under a dominant wind direction, is x_{i}, the time taken for the wind to propagate from the first wind farm x_1 to another wind farm x_{i} is defined as the time delay T, given by:

$$T = \frac{x_i - x_1}{v_{\text{travel}}} \tag{9}$$

Then, the wind speed at wind farm i located at x_{i} can be expressed as a function of the wind speed at the starting point:

$$v_{\text{wind},i}(t) = v_{\text{wind}}(x_1, t - \frac{x_i - x_1}{v_{\text{travel}}}) \tag{10}$$

To establish the relationship of power waveforms based on the above wind speed relationship, the power waveform of the first wind farm $P_{wind,1}(t)$ is defined as the representative power waveform along the dominant wind direction. Then, the power waveform $P_{wind,i}(t)$ of wind farm i can be expressed as a function of the representative power waveform:

$$P_{\text{wind},i}(t) = \frac{S_i}{S_1} P_{\text{wind},1}(t - \frac{x_i - x_1}{v_{\text{travel}}}) \tag{11}$$

B. OWF Cluster Power Considering Wind Direction Variations

A wind farm cluster consists of m wind farms, located in the geographical region Ω. To analyze the power fluctuation of the cluster, the wind farms can be treated as individual points, ignoring the internal dispersion of wind turbines within the region.

The aggregated power of multiple wind farms can be transmitted to remote load centers after being connected to the main power grid via the transmission system. The power waveform of the wind farm cluster under typhoon conditions is the total power waveform of all wind farms $P_{wind,1}(t)$.

$$P_{\text{cluster}}(t) = \sum_{t=1}^{m} P_{\text{wind,i}}(t) \tag{12}$$

where m is the number of wind farms in the cluster; $P_{wind,i}(t)$ is the nominal-value power waveform of wind farm i under typhoon conditions.

By substituting $P_{wind,i}(t)$ into Equation (12), the power waveform of the wind farm cluster can be expressed as:

$$P_{\text{cluster}}(t) = \sum_{i=1}^{m} \frac{S_i}{S_1} P_{\text{wind},1}(t - \frac{x_i - x_1}{v_{\text{travel}}}) \tag{13}$$

However, the power fluctuation characteristics of wind farm clusters are influenced by meteorological factors such as wind speed and wind direction as well as spatial distribution. Wind direction is not uniformly distributed in different directions, as shown in Fig. 2.

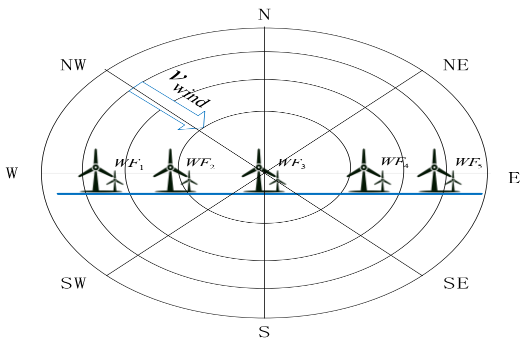

Fig.2 Wind direction rose chart of wind power clusters

To reflect the randomness of the wind direction, the fixed distance in the time delay needs to be replaced by the projected distance towards the prevailing wind direction. The effective downwind projection distance of wind turbine i relative to wind turbine 1 is:

$$L = (x_i - x_1)\cos\theta(t) + (y_i - y_1)\sin\theta(t) \tag{14}$$

In this paper, the time delay is defined with consideration of a dominant wind speed, and thus only the horizontal axis projection is taken into account. The original fixed delay is replaced with a wind direction-related dynamic delay:

$$T' = \frac{(x_i - x_1)\cos\theta(t)}{v_{\text{travel}}} \tag{15}$$

Assuming that the distance and capacity of each wind farm are L_d and S_{av} respectively, a cumulative model with equal distance and equal capacity is obtained:

$$P_{\text{cluster}}(t) = \sum_{i=1}^{m} P_{\text{wind},1}(t - \frac{(i-1)L_d\cos\theta_t}{v_{\text{travel}}}) \tag{16}$$

By substituting Equation (8) into (16), the power waveform of the wind farm cluster under typhoon conditions can be expressed as:

TABLE I
CORRELATIONS OF ACTUAL WIND POWER WAVEFORMS OF ADJACENT WIND FARMS

$P_1(t), P_2(t)$	$P_2(t), P_3(t)$	$P_3(t), P_4(t)$	$P_4(t), P_5(t)$	Average
0.86	0.76	0.70	0.89	0.80

979-8-3315-8138-1

$$P_{\text{cluster}}(t) = mP_{1,\text{const}} + \sum_{i=1}^{m} \delta_{\text{A},i} \sum_{q=1}^{s} P_{1,\text{q,max}} \, sin\left(2\pi f_q \left(t - \frac{(i-1)L_d \cos\theta_t}{v_{\text{travel}}}\right) - \theta_q\right) \quad (17)$$

IV. CASE STUDIES

This chapter takes three adjacent OWFs (each with an installed capacity of 400MW and 100 units of 4MW) in the sea area near the Three Gorges in Jiangsu as the research objects. They are approximately 13.7 kilometers apart from east to west and arranged linearly. The typical path and intensity of a typhoon are taken as the example scenario, with a time resolution of 15 minutes and a simulation span of 96 hours.

A. Model Comparison Results and Analysis

In this section, we compare the WDSA model with the conventional baseline model (BM) to validate the effectiveness of our approach. Fig.3 presents a comparison between the simulated results of both models and the actual measured power of wind power cluster SX.

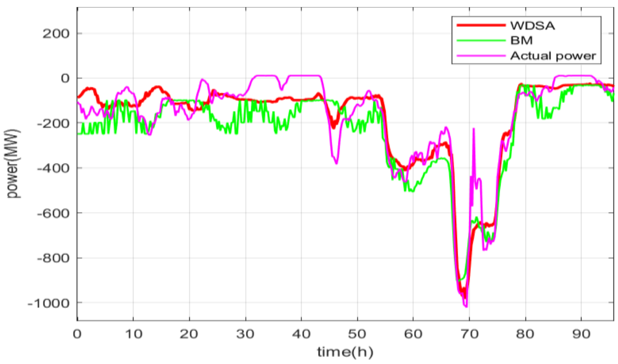

Fig. 3 Comparison of Power Curves for Wind Power Cluster SX

As shown in Fig.3, during the typhoon impact, the theoretical power converted from the wind speed-power curve indicates that wind turbines should be completely shut down when the wind speed theoretically exceeds the cut-out speed. However, in reality, wind farms continue to generate some power, causing the BM simulated power to fluctuate with the wind speed curve and resulting in significant deviations from the actual power. In contrast, the WDSA model accurately captures the smooth power decay and recovery process, and the overall RMSE increased by 4.32%.

B. Effectiveness Analysis of Wind Turbine Failure Model

As shown in Fig. 4, δ_A is a function of wind speed, and there is a negative correlation between the two. Different from the assumptions of traditional models, when the wind speed is lower than the wind turbine's cut-out wind speed (set to 30 m/s in this case), δ_A does not equal 1. Instead, it fluctuates slightly between 0.80 and 0.85 due to the probability of wind speed-related failure rates and the randomness of MCS. When the wind speed exceeds the cut-out wind speed, δ_A begins to drop sharply. The simulation curve verifies that the δ_A calculation model constructed in this paper, based on probability failure rates and MCS, can more realistically and precisely simulate the behavior of wind turbines under typhoon conditions, and reveals the probabilistic outage and fluctuation characteristics near the cut-out wind speed threshold.

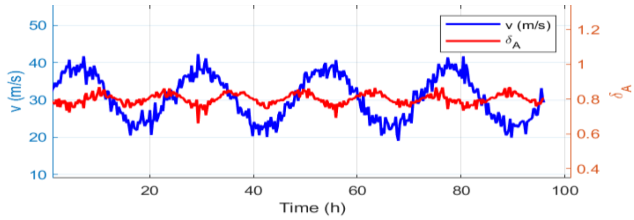

Fig. 4 Time Series of Wind Speed and Available Installed Capacity Factor

C. Ablation Experiment

To evaluate the performance of the complete WDSA model in this paper, comparison schemes 1, 2, and 3 are established as models considering frequency decomposition and spatiotemporal delay, frequency decomposition and available installed capacity, and spatiotemporal delay and available installed capacity, respectively, denoted as PM-FT, PM-FC, and PM-TC. Comparison schemes 4, 5, and 6 correspond to models considering only frequency decomposition, spatiotemporal delay, and available installed capacity, respectively, denoted as PM-F, PM-T, and PM-C.

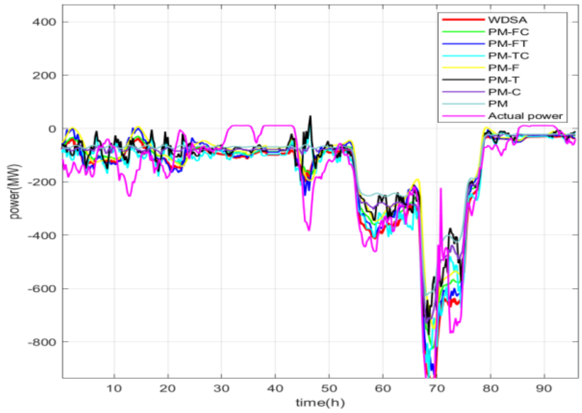

Fig. 5 Comparison of Power Curves for Different Simulation Schemes

TABLE II
COMPARISON OF ERRORS OF DIFFERENT CLUSTER POWER SIMULATION SCHEMES UNDER TYPHOON CONDITIONS(MW)

Model	RMSE	MAE	NRMSE
WDSA	76.527	59.154	7.41%
PM-FC	84.183	65.335	8.16%
PM-FT	90.205	70.154	8.74%
PM-TC	87.901	65.368	8.52%
PM-F	95.912	73.718	9.29%
PM-T	107.494	75.127	10.41%
PM-C	91.744	68.911	8.89%
PM	113.613	81.199	11.01%

As shown in Fig.5 and Table II, compared to the baseline model, the models integrating individual modules—PM-F, PM-T, and PM-C—achieved improvements to varying degrees across key metrics. From the perspective of dual-module synergy, the accuracy improvement achieved by combining any two modules is significantly greater than that of any single module, demonstrating clear complementary effects. Furthermore, the WDSA model, which integrates all three modules, leverages the frequency decomposition module to extract fundamental fluctuation characteristics of power, the spatiotemporal delay module to correct power phase differences among wind farms based on wind speed propagation patterns, and the available installed capacity module to provide realistic amplitude inputs for the phase-corrected power superposition. The synergy among the three modules further reduces the NRMSE to 7.41%, fully validating the core value of multi-module collaboration in enhancing the accuracy of cluster power simulation in typhoon scenarios.

D. Sensitivity Analysis

In actual wind farms, the atmospheric propagation conditions and the operating status of equipment change simultaneously and may exhibit interaction. To conduct an in-depth study of this combined influence, this section employs a three-dimensional sensitivity analysis method for the WDSA model. Taking frequency decomposition (f), wind direction delay (T), and AICC (c) as independent variables, and RMSE and correlation coefficient as evaluation indicators, pairwise coupling parameter analysis is conducted.

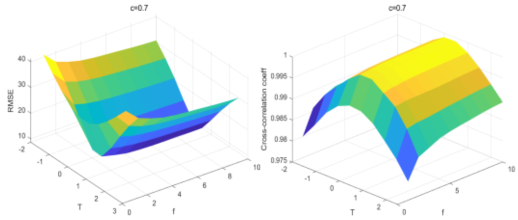

(a) Fixed AICC scenario

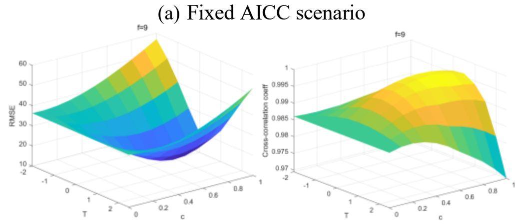

(b) Fixed frequency decomposition scenario

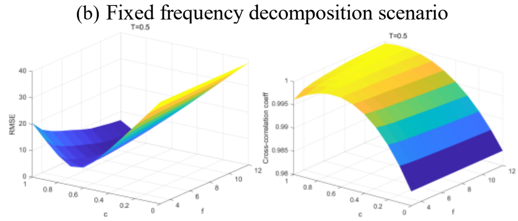

(c) Fixed wind direction delay scenario

Fig. 6 Sensitivity analysis of WDSA model

Fig.6 evaluates the impact of three parameters on the proposed model's performance through training error. When c is fixed, since low-frequency decomposition fails to adequately capture the high-frequency fluctuations in wind farm power while excessive frequency decomposition introduces wind farm noise interference, the results indicate that at a frequency decomposition of f=9, a wind direction time delay of T=0.5h achieves optimal phase matching of waveforms across wind farms, yielding the lowest RMSE and highest correlation coefficient. When T is fixed, similarly at f=9, the RMSE shows a clear pattern of first decreasing and then increasing with variations in c, reaching optimal model accuracy at c=0.7 where the available wind farm capacity aligns perfectly with the actual power output demand during the peak typhoon period. Finally, with f fixed at its optimal value, it is further verified that the parameter coupling achieves the best performance at T=0.5h and c=0.7. In summary, the optimal parameter combination is f=9, c=0.7, and T=0.5h, enabling the model to accurately capture fluctuation characteristics, match actual capacity requirements, and achieve phase synchronization of fluctuating components.

V. CONCLUSION

This paper proposes a WDSA model for analyzing the power fluctuations of OWF clusters in the scenario of typhoon. This model effectively depicts the uncertainties of the OWF shutdown state by constructing an AICC considering typhoon conditions. The parameter combines the model of wind speed failure rate and MCS. By introducing the projection distance of the wind direction to calculate the time delay, the power phase difference between different wind farms is corrected. The proposed model solves the error of time delay caused by the ignorance of spatial distribution in traditional aggregation methods. The model is verified through the actual output of wind power clusters in the sea areas near Jiangsu, demonstrating good accuracy and providing a mathematical view for the mechanism of OWF power fluctuation. The overall RMSE has increased by 4.32% compared with the traditional model. The proposed model helps the safe and stable operations of the modern power systems under extreme weathers.

ACKNOWLEDGMENT

This work is supported by National Key R&D Program of China “Remote monitoring and fault diagnosis technology for offshore wind power grid connected systems (2023YFB2406900)”.

REFERENCES

[1] M. Yang, L. Zhang, Y. Cui, Y. Zhou, Y. Chen and G. Yan, "Investigating the Wind Power Smoothing Effect Using Set Pair Analysis," in IEEE Transactions on Sustainable Energy, vol. 11, no. 3, pp. 1161-1172, July 2020.

[2] Z. Yang, X. Peng, J. Song, R. Duan, Y. Jiang and S. Liu, "Short-Term Wind Power Prediction Based on Multi-Parameters Similarity Wind Process Matching and Weighed-Voting-Based Deep Learning Model Selection," in IEEE Transactions on Power Systems, vol. 39, no. 1, pp. 2129-2142, Jan. 2024.

[3] F. Rong, G. Wu, X. Li, S. Huang and B. Zhou, "ALL-DC Offshore Wind Farm with Series-Connected Wind Turbines to Overcome Unequal Wind Speeds," in IEEE Transactions on Power Electronics, vol. 34, no. 2, pp. 1370-1381, Feb. 2019.

[4] Y. Fu, Y. Liu, L. -l. Huang, F. Ying and F. Li, "Collection System Topology for Deep-Sea Offshore Wind Farms Considering Wind Characteristics," in IEEE Transactions on Energy Conversion, vol. 37, no. 1, pp. 631-642, March 2022.

[5] D. Li, W. Yan, W. Li and Z. Ren, "A Two-Tier Wind Power Time Series Model Considering Day-to-Day Weather Transition and Intraday Wind Power Fluctuations," in IEEE Transactions on Power Systems, vol. 31, no. 6, pp. 4330-4339, Nov. 2016.

[6] M. Mehrjoo, M. J. Jozani, M. Pawlak and B. Bagen, "A Multilevel Modeling Approach Towards Wind Farm Aggregated Power Curve," in IEEE Transactions on Sustainable Energy, vol. 12, no. 4, pp. 2230-2237, Oct. 2021.

[7] W. Teng, X. Wang, Y. Meng and W. Shi, "An improved support vector clustering approach to dynamic aggregation of large wind farms," in CSEE Journal of Power and Energy Systems, vol. 5, no. 2, pp. 215-223, June 2019.

[8] P. Wang, Z. Zhang, Q. Huang, N. Wang, X. Zhang and W. -J. Lee, "Improved Wind Farm Aggregated Modeling Method for Large-Scale Power System Stability Studies," in IEEE Transactions on Power Systems, vol. 33, no. 6, pp. 6332-6342, Nov. 2018.

[9] Y. Jin, D. Wu, P. Ju, C. Rehtanz, F. Wu and X. Pan, "Modeling of Wind Speeds Inside a Wind Farm with Application to Wind Farm Aggregate Modeling Considering LVRT Characteristic," in IEEE Transactions on Energy Conversion, vol. 35, no. 1, pp. 508-519, March 2020.

[10] G. A. Orfanos, P. S. Georgilakis and N. D. Hatziargyriou, "Transmission Expansion Planning of Systems with Increasing Wind Power Integration," in IEEE Transactions on Power Systems, vol. 28, no. 2, pp. 1355-1362, May 2013.

979-8-3315-8138-1